Progress In Electromagnetics Research M, Vol. 45, 51–58, 2016

Microwave Focusing within Arbitrary Refractive Index Media Using Left-Handed Metamaterial Lenses

Luca Leggio*, Ehsan Dadrasnia, and Omar de Varona

Abstract—Left-handed metamaterial (LHM) lenses allow the focusing of microwave radiation at specific positions within a medium, depending on its refractive index. A suitable approach needs to consider the reflections between the LHM lens and the adjacent media. This work faces the challenge of focusing the microwave radiation within a medium with arbitrary positive refractive index and characteristic impedance using LHM lenses as imaging-forming systems. To find a right lens formula a full wave method is presented in theory. The results we achieved show that the characteristic flat shape of conformal-four lens configuration has a spot size of $0.53 \times 0.34\lambda_{eff}^2$ at $-3\,\mathrm{dB}$ if the different media are perfectly matched. Otherwise, a noteworthy aberration affects the focusing, but it can be mitigated using a conformal circular LHM lens with a spot size of $\sim 0.4 \times 0.4\lambda_{eff}^2$ at $-3\,\mathrm{dB}$.

1. INTRODUCTION

Negative refractive index media have been debated for the first time by Veselago [1] to describe the impact upon basic electromagnetic phenomena: the inversion of the electromagnetic waves propagation and of phase velocity vector, the resolution below diffraction limit, the inversion of Cherenkov radiation and Doppler's effect. One of the most recent effects of this impact is the possibility to build special lenses based on the negative refraction, as reported by J. B. Pendry in [2], by asserting a flat slab of negative refractive index that behaves as a perfect lens. He presented a mathematical theory for this kind of lenses, which are supposed to be lossless and dispersiveless, to focus images with a better resolution (so called "superresolution") than its positive index lenses counterparts. Afterwards, a doubt on this theory has been raised for the analysis of evanescent waves in a left-handed metamaterial embedded between two positive refractive index media [3]. In this case, the amplification of evanescent waves is limited to a determinate width of the LHM lens, over which a non-ideal field focusing occurs. In addition, the inevitable absorption effect existing in real LHM lenses, fabricated with lossy metals, precludes the amplification of evanescent waves and is responsible for the focal shift [4].

References [5, 6] have discussed that at small wavelengths the resolution of a LHM lens (or "superlens") is independent from the absorption if both $\mathrm{Im}\varepsilon < 1$ and $\mathrm{Im}\mu < 1$. A new universal parameter (which relates wavelength, lens thickness, and absorption) imposes the conditions for having a superresolution of LHM lenses, remarking the transition with the diffraction-limited resolution. The implementation of LHM lenses composed of periodic arrays of artificial inclusions (metallic wires and split-rings resonators) has been applied using much shorter size than the operating wavelength, in order to achieve a bulk medium with negative effective permittivity and permeability [7–9], in which the image resolution is considerably reduced as the thickness of the LHM superlens increases [7]. Metamaterial lenses cover an interesting role in microwave hyperthermia treatment of tumors, as demonstrated in [10]. We have recently reported [11] the simulated behaviour of three different LHM lens configurations to focus the microwave radiation within a single-layer biological tissue: single-lens, double-lens and

Received 28 July 2015, Accepted 1 December 2015, Scheduled 16 December 2015
* Corresponding author: Luca Leggio (lleggio@ing.uc3m.es).
The authors are with Department of Electronic Technology, University of Carlos III, Madrid, Spain.

conformal four-lens. The conformal four-lens system has been proved to be the most performant in terms of focusing resolution, considering a perfect matching between media and a low-losses LHM lens.

Besides, Tassin et al. reported a LHM lens embedded between two media with same refractive index and characteristic impedance and derived the corresponding lens formula by a full wave method [12]. However, they have not taken into account a LHM lens between two media with different refractive index and characteristic impedance.

In this new work, we study a full wave method to find the suitable LHM lens formula using CST simulations. The results are demonstrated to agree with the pre-calculated numerical values.

Firstly, we show the determination of the focal distance with perfect refractive index and characteristic impedance matching between media (medium 1, LHM lens, and medium 2) using a conformal four-lens configuration with low-losses. The focusing spot is well-defined. Afterwards, we test the case of mismatching denoting the effect of focusing aberration due to the reflections between media. Furthermore, a conformal circular LHM lens is demonstrated to mitigate the focusing aberrations and a clearer spot is achieved. Finally, we analyse the frequency-dependent behaviour of the focal distance.

This study is organized into three sections. Section 2 presents the theoretical full wave method to obtain the focal distance using a flat LHM lens. Section 3 shows the results based on the proposed theory and some considerations on the fabrication of LHM lenses. Finally, Section 4 concludes the perspectives of this study.

2. THEORY AND ANALYSIS

The LHM lens potentially reproduces the source in the image plan below the limit of diffraction with high resolution. For this purpose, the full wave method proposed by Tassin can be used to calculate the LHM lens focal distance [12]. The full wave method takes into account the contrast between refractive indices and characteristic impedances of adjacent media, which produces reflections and a focusing aberration. A flat LHM lens with length L, refractive index $n_M < 0$ and characteristic impedance η_M is located between two media with refractive indices $n_1 > 0$ and $n_2 > 0$ and characteristic impedances η_1 and η_2, respectively. Neither the characteristic impedance nor the refractive index is matched, so that $n_1 \neq |n_M| \neq n_2$ and $\eta_1 \neq \eta_M \neq \eta_2$. Figure 1 shows a schematic flat LHM lens between two different media. In this scheme, the microwave source S (half-wave antenna) is located in the medium with refractive index n_1 and is placed at $z = 0$ on the propagation axis z.

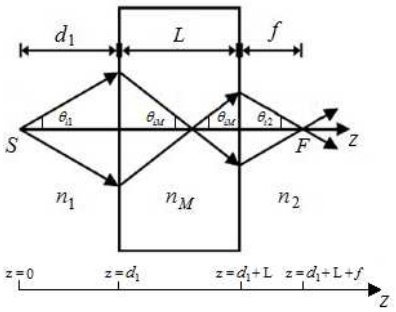

Figure 1. The scheme of microwave source behind a flat LHM lens. *Reprinted from Ref. [2].*

The aforementioned method considers the LHM lens as a Fabry-Pérot resonator [12] filled with a left-handed metamaterial. We calculate the transmission coefficient of the LHM lens when it is illuminated by a monochromatic plane wave. It is assumed that the wave incident on the lens surface is partially reflected and partially transmitted, as in a realistic scenario, and is TE polarized.

In order to obtain the transmittance of the system, the boundary conditions are applied at the interfaces. At $z = d_1$ we consider the continuity of electric field and of the tangential components of magnetic field that yields the following equations, respectively:

$$E_{0i1}e^{ikd_1} + E_{0r1}e^{-ikd_1} = E_{0iM}e^{i\kappa d_1} + E_{0rM}e^{-i\kappa d_1}, \tag{1}$$

$$\eta_1 \cos\theta_{i1}\left(E_{0i1}e^{ikd_1} - E_{0r1}e^{-ikd_1}\right) = \eta_M \cos\theta_{iM}\left(E_{0iM}e^{i\kappa d_1} - E_{0rM}e^{-i\kappa d_1}\right), \tag{2}$$

where E_{0i1}, E_{0r1}, E_{0iM}, E_{0rM} are the amplitudes of the electric field (incident and reflected) in medium 1 and in the LHM lens, respectively. θ_{i1} and θ_{iM} are the incidence angles of the electromagnetic wave in the medium 1 and in the LHM lens, respectively, $k = \frac{\omega}{c} n_1 \cos\theta_{i1}$ and $\kappa = \frac{\omega}{c} n_M \cos\theta_{iM}$, where ω is the angular frequency of electromagnetic field and c is the speed of light. Eq. (2) can be rewritten replacing $\varsigma = \eta_1 \cos\theta_{i1}$ and $\xi = \eta_M \cos\theta_{iM}$ as follows:

$$E_{0i1} e^{ikd_1} - E_{0r1} e^{-ikd_1} = \frac{\xi}{\varsigma} \left(E_{0iM} e^{i\kappa d_1} - E_{0rM} e^{-i\kappa d_1} \right). \tag{3}$$

To eliminate the second term, we get the summation of Eqs. (1) and (3):

$$2\varsigma E_{0i1} e^{ikd_1} = (\xi + \varsigma) E_{0iM} e^{i\kappa d_1} - (\xi - \varsigma) E_{0rM} e^{-i\kappa d_1}. \tag{4}$$

The same boundary conditions must also be fulfilled at $z = L + d_1$. The continuity of the electric and magnetic fields at the second interface yields the following equations, respectively:

$$E_{0iM} e^{i\kappa(L+d_1)} + E_{0rM} e^{-i\kappa(L+d_1)} = E_{0t2} e^{i\psi(L+d_1)}, \tag{5}$$

$$E_{0iM} e^{i\kappa(L+d_1)} - E_{0rM} e^{-i\kappa(L+d_1)} = \frac{\beta}{\xi} E_{0t2} e^{i\psi(L+d_1)}, \tag{6}$$

where E_{0t2} is the electric field transmitted in the medium 2, $\psi = \frac{\omega}{c} n_2 \cos\theta_{t2}$, $\beta = \eta_2 \cos\theta_{t2}$, and θ_{t2} is the incidence angle of the electromagnetic wave in the medium 2. Summing the expressions (5) and (6), we get the following equations:

$$E_{0iM} e^{i\kappa d_1} = \left(\frac{\xi + \beta}{2\xi} \right) E_{0t2} e^{i\psi(L+d_1)} e^{-i\kappa L}, \tag{7}$$

$$E_{0rM} e^{-i\kappa d_1} = \left(\frac{\xi - \beta}{2\xi} \right) E_{0t2} e^{i\psi(L+d_1)} e^{i\kappa L}. \tag{8}$$

The transmission coefficient t can be derived by replacing (7) and (8) in Eq. (4) as follows:

$$t = \frac{E_{0t2}}{E_{0i1}} = \frac{4\xi\varsigma e^{ikd_1} e^{-i\psi(L+d_1)}}{(\varsigma + \xi)(\xi + \beta) e^{-i\kappa L} - (\xi - \varsigma)(\xi - \beta) e^{i\kappa L}}, \tag{9}$$

where the real and imaginary parts of the denominator are:

$$\mathrm{Re}\left((\varsigma + \xi)(\xi + \beta) e^{-i\kappa L} - (\xi - \varsigma)(\xi - \beta) e^{i\kappa L} \right) = 2(\varsigma\xi + \xi\beta)\cos(\kappa L), \tag{10}$$

$$\mathrm{Im}\left((\varsigma + \xi)(\xi + \beta) e^{-i\kappa L} - (\xi - \varsigma)(\xi - \beta) e^{i\kappa L} \right) = -2\left(\xi^2 + \varsigma\beta\right)\sin(\kappa L), \tag{11}$$

These give us the module and argument of denominator of (9) as indicated below:

$$\left| (\varsigma + \xi)(\xi + \beta) e^{-i\kappa L} - (\xi - \varsigma)(\xi - \beta) e^{i\kappa L} \right| = 2\sqrt{(\varsigma\xi + \xi\beta)^2 + (\xi^4 + \varsigma^2\beta^2 - \varsigma^2\xi^2 - \xi^2\beta^2)\sin^2(\kappa L)}, \tag{12}$$

$$\angle\left((\varsigma + \xi)(\xi + \beta) e^{-i\kappa L} - (\xi - \varsigma)(\xi - \beta) e^{i\kappa L} \right) = -\frac{\left(\xi^2 + \varsigma\beta\right)}{(\varsigma\xi + \xi\beta)} \tan(\kappa L). \tag{13}$$

Therefore, the transmission coefficient in (9) can be rewritten as follows:

$$t = \frac{E_{0t2}}{E_{0i1}} = \frac{2\xi\varsigma e^{ikd_1} e^{-i\psi(L+d_1)} e^{i \arctan\left(\frac{\left(\xi^2 + \varsigma\beta\right)}{(\varsigma\xi + \xi\beta)} \tan(\kappa L) \right)}}{\sqrt{(\varsigma\xi + \xi\beta)^2 + (\xi^4 + \varsigma^2\beta^2 - \varsigma^2\xi^2 - \xi^2\beta^2)\sin^2(\kappa L)}}. \tag{14}$$

Equation (14) already takes into account the propagation term e^{ikd_1} from $z = 0$ to $z = d_1$. To represent the impulse response of the whole system from object to image point, the propagation term $e^{i\psi f}$ from $z = L + d_1$ to $z = L + d_1 + f$, where f is the focal distance in medium 2, has to be included. Hence, the impulse response H can be expressed as:

$$H = \frac{E_{0t2}}{E_{0i1}} e^{i\psi f} = \frac{2\xi\varsigma e^{ikd_1} e^{i\psi f} e^{i \arctan\left(\frac{\left(\xi^2 + \varsigma\beta\right)}{(\varsigma\xi + \xi\beta)} \tan(\kappa L) \right)}}{\sqrt{(\varsigma\xi + \xi\beta)^2 + (\xi^4 + \varsigma^2\beta^2 - \varsigma^2\xi^2 - \xi^2\beta^2)\sin^2(\kappa L)}}. \tag{15}$$

In the last equation, the negative phase term $e^{-i\psi(L+d_1)}$ has been removed because is related to backward propagation. The phase of the impulse response is described by:

$$\varphi = d_1 k + f\psi + \arctan\left(\left(\frac{\xi^2+\zeta\beta}{\zeta\xi+\xi\beta}\right)\tan(\kappa L)\right), \tag{16}$$

where: $\zeta = k/\mu_1$, $\xi = \kappa/\mu_M$, and $\beta = \psi/\mu_2$, considering $k = \sqrt{\frac{\omega^2 n_1^2}{c^2} - k_x^2 - k_y^2}$, $\kappa = -\sqrt{\frac{\omega^2 n_M^2}{c^2} - k_x^2 - k_y^2}$, and $\psi = \sqrt{\frac{\omega^2 n_2^2}{c^2} - k_x^2 - k_y^2}$. The derivative of this term $d\varphi/d(k_x^2+k_y^2)|_{k_x^2+k_y^2=0} = 0$ gives the focal distance f at which the image point is located:

$$f = \frac{Ln_2\left(|n_M|^2 + n_1 n_2\right) Sec^2\left(L\,|n_M|\,\omega/c\right)}{|n_M|^2\,(n_1+n_2)\,(1+A^2 Tan^2\,(L\,|n_M|\,\omega/c))} - \frac{B\frac{c}{\omega}Tan\,(L\,|n_M|\,\omega/c)}{(1+A^2 Tan^2\,(L\,|n_M|\,\omega/c))} - \frac{n_2}{n_1}d_1, \tag{17}$$

where: $A = \frac{|n_M|^2+n_1 n_2}{|n_M|(n_1+n_2)}$, $B = \frac{(n_1^2-|n_M|^2)(n_2^2-|n_M|^2)}{|n_M|^3(n_1+n_2)n_1}$, with $\mu_1 = 1$, $\mu_M = -1$ and $\mu_2 = 1$. It can be noticed that the focal distance is a frequency-dependent function [see Eq. (17)]. The second term tends to 0 towards several hundreds of GHz.

3. RESULTS AND DISCUSSION

To test the aforementioned theory in Section 2, the mismatching and perfect matching conditions are considered in separate cases. We apply a conformal four-lens system to produce an enhanced focusing [11]. Each medium involved in the simulations is assumed as non-magnetic [12].

3.1. Perfect Matching

In this case, a perfect refractive index and characteristic impedance matching between media are considered: $n_1 = |n_M| = n_2$ and $\eta_1 = \eta_M = \eta_2$. The thickness of the conformal four-lens system is $L = 6\,\text{cm}$ and the distance between each antenna from the correspondent LHM lens is $d_1 = 3\,\text{cm}$. The operation frequency is at 6 GHz, where each antenna is half-wave. This length needs to be sufficiently small in order to have right propagation direction inside the LHM lens. Table 1 presents the characteristics of media considered in the simulation at 6 GHz. The media have the refractive indices of $n_1 = 3$, $n_M = -3$, and $n_2 = 3$ [11]. The LHM lens is studied as an effective isotropic medium characterized using the Drude model for both the relative permittivity ε_{rLHM} and permeability μ_{rLHM}, as follows:

$$\varepsilon_{rLHM}(\omega) = 1 - \frac{\omega_{pe}^2}{\omega^2 + 2j\delta\omega}, \tag{18}$$

$$\mu_{rLHM}(\omega) = 1 - \frac{\omega_{pm}^2}{\omega^2 + 2j\delta\omega}, \tag{19}$$

where δ is the collision frequency, and ω_{pe} and ω_{pm} are respectively the electrical and magnetic plasma frequencies. In this example, $\omega_{pe} \approx 119.215\cdot 10^9\,\text{rad/s}$, $\omega_{pm} \approx 53.315\cdot 10^9\,\text{rad/s}$ and $\delta = 1.0048\cdot 10^8\,\text{rad/s}$ are replaced in Eqs. (18) and (19) for the LHM lens [11]. From Eq. (17), the focal distance is obtained ($f = 3\,\text{cm}$), in which the focusing spot should be located in the middle of the material with refractive

Table 1. The electromagnetic parameters of medium 1, LHM lens, and medium 2 at 6 GHz [11].

Material	Refractive Index	Relative Permittivity	Relative Permeability
Medium 1	3.0	9.0	1.0
LHM Lens	−3.0	−9.0	−1.0
Medium 2	3.0	9.0	1.0

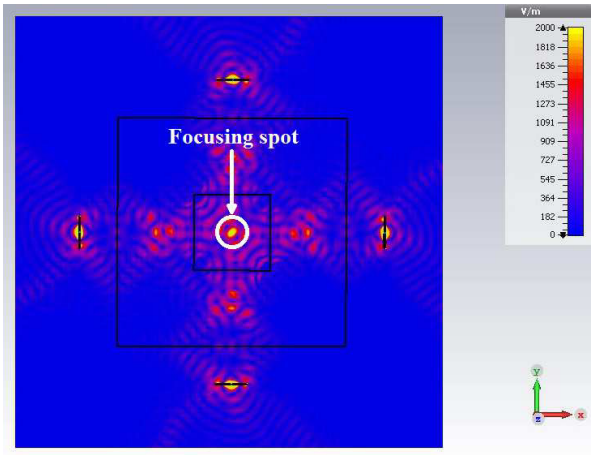

Figure 2. The microwave focusing in a medium in conditions of perfect matching between media.

index n_2. Figure 2 demonstrates the CST simulation in which the E-field focusing occurs in the expected focal point. The focusing only involves a spot whose size is slightly elliptical, due to the effect of the corners of square shape, and is roughly $0.53 \times 0.34\lambda_{eff}^2$ at -3 dB, where λ_{eff} is the effective wavelength is medium 2 ($\lambda_{eff} = \lambda/n_2$).

3.2. Mismatching

In this example, we consider $n_1 \neq |n_M| \neq n_2$ and $\eta_1 \neq \eta_M \neq \eta_2$. Again, $L = 6$ cm, $d_1 = 3$ cm and the operation frequency is 6 GHz. Table 2 presents the characteristics of the media considered in the simulation. The media have the refractive indices of $n_1 = 1.56$, $n_M = -2$, and $n_2 = 3$. With a similar approach to Section 3.1, for the LHM lens the Drude model described in Eqs. (18) and (19) is followed for both permittivity and permeability with the parameters of $\omega_{pe} \approx 84.298 \cdot 10^9$ rad/s, $\omega_{pm} \approx 53.315 \cdot 10^9$ rad/s and $\delta = 1.0048 \cdot 10^8$ rad/s.

Table 2. The electromagnetic parameters of medium 1, LHM lens, and medium 2 at 6 GHz.

Material	Refractive Index	Relative Permittivity	Relative Permeability
Medium 1	1.56	2.434	1.0
LHM Lens	-2.0	-4.0	-1.0
Medium 2	3.0	9.0	1.0

Following Eq. (17), the focal distance is located at $f \approx 3$ cm, which is in the middle of the material with refractive index n_2. As demonstrated in Figure 3 by a CST simulation, the E-field focusing occurs in the calculated focus. The focusing particularly involves a broader area, because of the contrast between different refractive indices that produces spherical aberrations [13]. This area is increasing with the contrast between refractive indices. Figure 3 shows a central spot ($0.36 \times 0.33\lambda_{eff}^2$ at -3 dB) containing the major contribution of the electromagnetic power and eight surrounding spots with smaller size and lower power.

3.3. Discussion

The focal distance is a frequency-dependent function in Eq. (17), as demonstrated in Figure 4. The dependency of the focal distance is presented in the range between 1 and 100 GHz for both above scenarios of mismatching (in blue) and perfect matching between media (in red). In both cases, $L = 6$ cm and $d_1 = 3$ cm to get a focal distance $f = 3$ cm at 6 GHz. The numerical values in Tables 1 and 2 have been applied for each case. It can be seen that the focal distance is constant in perfect matching with

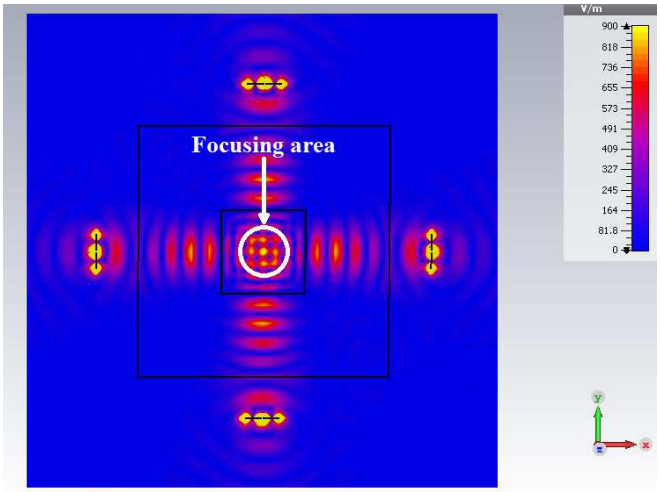

Figure 3. The microwave focusing in a medium with arbitrary refractive index using a four-lens system.

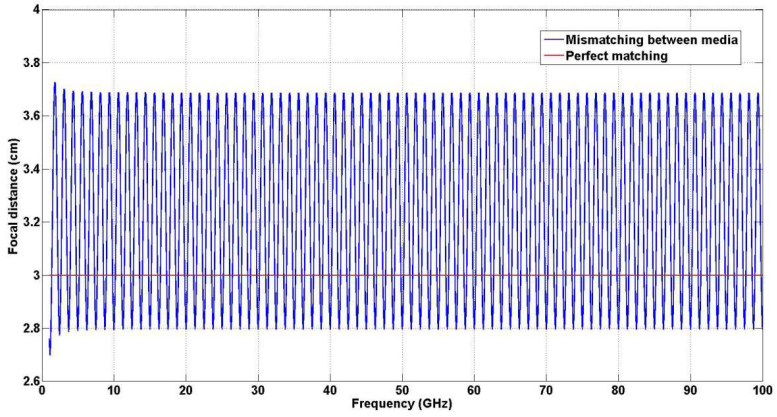

Figure 4. The focal distance as function of frequency is illustrated for the mismatching case (blue line). The oscillating behaviour is due to frequency-dependent reflections. The independent-frequency focal distance is illustrated for the case of perfectly matched media (red line).

the parameters of Table 1, considering $L = 6\,\text{cm}$ and $d_1 = 3\,\text{cm}$. The focal distance oscillates between $\sim 2.8\,\text{cm}$ and $\sim 3.7\,\text{cm}$ with a frequency of $\sim 1.25\,\text{GHz}$ in mismatching. These values depend on both the refractive indices and characteristic impedances which may take the reflection effects. The aberration effect noticed in Figure 3 can be reduced by using circular shapes of LHM lenses.

Figure 5 demonstrates a focusing of microwave radiation using a conformal circular lens surrounding the medium 2, considering the same parameters used in 3.2. There is a well-defined central spot whose size is $\sim 0.4 \times 0.4\lambda_{eff}^2$ at $-3\,\text{dB}$. However, in contrast to Figure 3, the aberrations around the central spot are gradually reduced. This proves that the circular LHM lenses allow attaining clear focusing spot shapes with low aberration. The high intrinsic losses represent the main complication that limits the practical implementation of LHM lenses and affects the focusing resolution. As the fabrication of LHM lenses with low losses and high power transfer is very hard, a loss compensation technique increasing the inductance to capacitance ratio and figure of merit of a LHM structure has been proposed [14].

In the experimental configuration, the LHM lenses can be implemented with arrays of sub-wavelength resonating structures (split-ring resonators and thin wires) [7], but they have considerable losses. For this purpose, an ultra-low loss split-ring resonator (SRR) has been proposed [15]. This approach incorporates lumped/interdigital capacitors or a dielectric medium into the SRR (SRR-

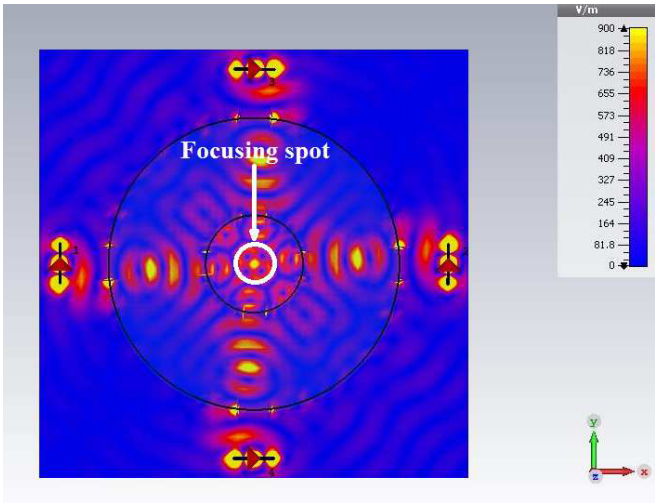

Figure 5. The microwave focusing is noticeably improved using a conformal circular LHM lens.

LC/SRR-IDC or SRR-die) with the purpose of redistributing the surface currents of the loop.

The near-field LHM lenses are mainly applicable to biomedical imaging and scanning [16, 17], while the far-field ones are mostly applied to antenna gain enhancement [18, 19]. For small thicknesses of LHM lenses, the losses are negligible. If a far-field focusing is desired, then the LHM lens thickness should be increased. Nevertheless, over a certain thickness, the LHM lenses exhibit losses and the evanescent waves decay away. To achieve this, a far-field superlens by adding a subwavelength silver-dielectric multilayer on the original silver superlens at optical wavelengths has been proposed [20]. This kind of lenses can increase the evanescent waves converting them into propagating waves projected in the far-field. The LHM lenses discussed are normally implemented for near-field imaging purposes [21, 22], but the thickness can be extended for achieving far-field focusing. A potential application of LHM lenses discussed in this work is the detection and imaging of small targets located in depth [16, 17]. In our simulations we have used ideal low-losses LHM lenses whose size ($L = 6\,\text{cm}$) allows achieving a focus (at $f = 3\,\text{cm}$) in near-field region: $f < 2l^2/\lambda_{eff} = \lambda n_2/2 = 7.5\,\text{cm}$, where l is the linear dimension of the antenna and λ is the wavelength in vacuum.

4. CONCLUSIONS

In this work, we have demonstrated simplified relations to adjust the focusing within a material with arbitrary refractive index. We have demonstrated the full wave method using CST simulations by taking into account the reflections between media. To simplify the equations, we have considered non-magnetic media. The results shown are in agreement with the calculated values. By using a flat conformal four-lens configuration, a perfect focusing has been achieved inside the inner medium in conditions of perfect refractive and impedance matching between media. Contrarily, focusing aberrations have occurred in the case of mismatching. This is due to contrast between refractive indices. The circular LHM lens shapes can moderate the aberration effect. We have also proved that the frequency variation of the focal distance depends on the reflections between media. The full wave method applied in this work is potentially extendible to a multi-layer case, but the increase of LHM lens thickness would increase the losses and the reflections between media. Additionally, a stronger aberration would unavoidably occur. This will happen especially if the objective is to focus the radiation on a multi-layered biological tissue that is particularly lossy. The losses of "superlens" have not been investigated in this work, since the aim was only to demonstrate the microwave focusing. However, the LHM lenses proposed are oriented to study the microwave radiation at longer distances. The research on LHM superlenses has shown a growing interest in practical applications, such as: biomedical imaging and treatment of tumors, antenna gain enhancement, and lithography. For future research, the low-losses LHM lenses should be investigated more in depth for far-field focusing.

REFERENCES

1. Veselago, V. G., "The electrodynamics of substances with simultaneously negative values of ε and μ," *Soviet Physics Uspekhi*, Vol. 10, No. 4, 509–14, 1968.
2. Pendry, J. B., "Negative refraction makes a perfect lens," *Physical Review Letters*, Vol. 85, No. 18, 3966–3969, 2000.
3. Garcia, N. and M. Nieto-Vesperinas, "Left-handed materials do not make a perfect lens," *Physical Review Letters*, Vol. 90, No. 22, 229903, 2003.
4. Zhang, K.-K., H.-L. Luo, and S.-C. Wen, "Focal shift of paraxial gaussian beams in a left-handed material slab lens," *Chinese Physics Letters,* Vol. 27, No. 7 , 4774–4784, 2010.
5. Kuhta, N. A., V. A. Podolskiy, and A. L. Efros, "Far field imaging by a planar lens: diffraction versus superresolution," *Physical Review B*, Vol. 76, 205102, 2007.
6. Kuhta, N. A., V. A. Podolskiy, and A. L. Efros, "Quantifying the limitations of far-field imaging by a left-handed planar lens," *URSI General Assembly*, Chicago, 2008.
7. Aydin, K. and E. Ozbay, "Left-handed metamaterial based superlensfor subwavelength imaging of electromagnetic waves," *Applied Physics A*, Vol. 87, No. 2, 137–141, 2007.
8. Petrov, R. V., G. Srinivasan, M. I. Bichurin, and D. Viehland, "Three-dimensional left-handed material lens," *Applied Physics Letters*, Vol. 91, 104103, 2007.
9. Ozbay, E. and K. Aydin, "Negative refraction and subwavelength focusing using left-handed composite metamaterials," *Proceedings SPIE, Metamaterials III, Lensing I*, Vol. 6987, April 23, 2008.
10. Wang, G., Y. Gong, and H. J. Wang, "Schemes of microwave hyperthermia by using flat left-handed material lenses," *Microwave and Optical Technology Let.*, Vol. 51, No. 7, 1738–1743, 2009.
11. Leggio, L., O. de Varona, and E. Dadrasnia, "A comparison between different schemes of microwave cancer hyperthermia treatment by means of left-handed metamaterial lenses," *Progress In Electromagnetics Research*, Vol. 150, 73–87, 2015.
12. Tassin, P., I. Veretennicoff, and G. Van der Sande, "Veselago's lens consisting of left-handed materials with arbitrary index of refraction," *Optics Communications*, Vol. 264, 130–134, 2006.
13. Born, M. and E. Wolf, *Principles of Optics*, Seventh Edition, Cambridge University Press, 2002.
14. Zhou, J., T. Koschny, and C. M. Soukoulis, "An efficient way to reduce losses of left-handed metamaterials," *Optics Express*, Vol. 16, No. 15, 11147–11152, 2008.
15. Zhu, L., F. Meng, F. Zhang, J. Fu, Q. Wu, X. Ding, and J. L.-W. Li, "An ultra-low loss split ring resonator by suppressing the electric dipole moment," *Progress In Electromagnetics Research*, Vol. 137, 239–254, 2013.
16. Fang, J., G. Yu, H. Wang, and W. Gang, "Study on near field target detection and imaging by using flat LHM lens," *META08–Proceed. of the 2008 Intern. Workshop on Metamaterials*, November 9–12, 2008.
17. Wang, G., J. Fang, and X. Dong, "Resolution of near-field microwave target detection and imaging by using flat LHM lens," *IEEE Transactions on Antennas and Propagation*, Vol. 55, No. 12, 3534–3541, 2007.
18. Turpin, J. P., Q. Wu, D. H. Werner, B. Martin, M. Bray, and E. Lier, "Low cost and broadband dual-polarization metamaterial lens for directivity enhancement," *IEEE Transactions on Antennas and Propagation*, Vol. 60, 5717–5726, Dec. 2012.
19. Meng, F. Y., Y. L. Lyu, K. Zhang, Q. Wu, and L. W. Li, "A detached zero index metamaterial lens for antenna gain enhancement," *Progress In Electromagnetics Research*, Vol. 132, 463–478, 2012.
20. Zhang, X. and Z. Liu, "Superlenses to overcome the diffraction limit," *Nature Materials*, Vol. 7, 435–441, 2008.
21. Lan, L., W. Jiang, and Y. Ma, "Three dimensional subwavelength focus by a near-field plate lens," *Applied Physics Letters*, Vol. 102, No. 23, 231119, 2013.
22. Grbic, A., L. Jiang, and R. Merlin, "Near-field plates: Sub-diffraction focusing with patterned surfaces," *Science*, Vol. 320, No. 5875, 511–513, 2008.